

# Fabrication of carbon nanostructures using electron beam lithography and pyrolysis for biosensing applications

이정아<sup>†</sup> · 이광철<sup>\*</sup> · 박세일<sup>\*</sup>, 이승섭<sup>\*\*</sup>

## 전자빔 리소그래피와 열처리를 이용한 탄소 나노구조물의 제작 및 바이오센싱 응용연구

Jung A Lee, Kwang-Cheol Lee, Se Il Park, Seung S. Lee

**Key Words :** Carbon nanostructures(나노구조물), Pyrolysis(열처리), electron beam lithography(전자빔 리소그래피), 바이오센서(바이오센서)

### Abstract

We present a facile, yet versatile carbon nanofabrication method using electron beam lithography and resist pyrolysis. Various resist nanopatterns were fabricated using a negative electron beam resist, SAL-601, and were then subjected to heat treatment in an inert atmosphere to obtain carbon nanopatterns. Suspended carbon nanostructures were fabricated by wet-etching of an underlying sacrificial oxide layer. Free-standing carbon nanostructures, which contain 122 nm-wide, 15 nm-thick, and 2  $\mu\text{m}$ -long nanobridges, were fabricated by resist pyrolysis and nanomachining processes. Electron beam exposure dose effects on resist thickness and pattern widening were studied. The thickness of the carbon nanostructures was thinned down by etching with oxygen plasma. An electrical biosensor utilizing carbon nanostructures as a conducting channel was studied. Conductance modulations of the carbon device due to streptavidin-biotin binding and pH variations were observed.

### 1. Introduction

Detection of chemical or biological species using micro- or nanofabricated sensors is currently receiving great attention. In the case of mechanical sensors, micro- or nanocantilever bending or resonance frequency changes are monitored by embedded piezoresistors, piezoelectric materials, or strain-sensitive field effect transistors (FETs) [1-3]. Electrical sensors for gas or biomolecule detection were demonstrated using semiconductor or polymer nanowires, nanotubes, and

batch-fabricated silicon FETs [4-6].

Various nanofabrication methods have been pursued for nanodevices and nanoelectromechanical systems (NEMS), as well as for biosensors. Nanomaterial-based devices have active areas below a few tens of nm (down to the single molecule level), which are difficult to obtain by top-down fabrication techniques. In addition to the potential of integrated nano- and molecular devices, nanomaterial-based devices have unique properties such as ballistic transport, single crystallinity, and quantum phenomena. Despite the promising advantages of nanomaterial-based devices, there are ongoing technological challenges in their manufacture, such as large-scale integration and repeatability.

Silicon or top-down nanofabrication methods have excellent characteristics such as well-established material properties and processes. Although silicon nanodevices have advantages such as batch-fabrication and large-scale integration, increasing process complexity and

---

<sup>†</sup> 회원, 한국표준과학연구원

E-mail : sihwa2@kriss.re.kr

TEL : (042)868-5707 FAX : (02)123-1234

<sup>\*</sup> 한국표준과학연구원, 나노소자연구단

<sup>\*\*</sup> 한국과학기술원, 기계공학과

expensive process equipment for high fidelity pattern transfer are needed as feature sizes continue to decrease. Low-cost batch-fabrication of free-style, free-standing nanostructures can improve existing nanomaterial- and silicon-based devices and therefore broaden future nanotechnology applications.

Carbon thin film, which is fabricated by pyrolysis of patterned resist, shows amorphous graphite-like characteristics with tunable conductivity via pyrolysis temperatures [7]. Because the carbon film is fabricated through a lithography process, we can obtain free-handed micro- or nanostructures on a silicon substrate, where the feature size is limited by top-down lithography techniques. While the electrochemical behaviors of carbon films in applications such as microbatteries and molecular electronics have been demonstrated, utilization of their mechanical and electrical properties, especially overhanging nanostructures for sensor and actuator applications, is rarely reported [8, 9].

The minimum resistivity of carbon films obtained from resist pyrolysis approaches a few  $m\Omega\cdot\text{cm}$ , which is comparable to highly-doped polysilicon resistivity. Resistivity tailoring, from semi-insulating to conducting, is achieved simply by varying pyrolysis temperatures and chemical composition. In conventional NEMS devices, nanostructures are fabricated by etch or deposition steps using photo- or electron beam resists as masks. The characteristics of pattern transfer fidelity through the resist mask, such as etch selectivity, anisotropy, and etch rate, are important features in NEMS and semiconductor processes. Resists are also used in sacrificial layers as an alternative to silicon oxide in order to fabricate free-standing devices using surface micromachining technology. Resist masks or sacrificial layers are removed by strong acids, solvents, or oxygen plasmas. Resist strip and wafer cleaning are sometimes difficult, especially for a thick resist such as SU-8. The resist itself can be utilized as an active mechanical element in nanoscale devices. With this method, mechanical nanoscale components are fabricated without the necessity for additional deposition and etch processes.

In this paper, we present the fabrication of versatile carbon nanostructures derived from electron beam resist for various sensor and actuator applications, as well as their utilization in biosensors. Various resist shapes, including nanowires and nanodots, were patterned using a negative electron beam resist, SAL-601 (Shipley Co.), and a modified scanning electron microscope. The nanofabrication method eliminates additional processes such as reactive ion etching and provides batch-fabricated, low-cost nanodevices. We also demonstrate streptavidin-biotin binding and pH dependent conductance modulation using pyrolyzed carbon nanowire devices for biosensors.

## 2. Device Fabrication

### 2.1 Fabrication processes

Fig. 1 shows schematic views of the electrical biosensor utilizing carbon nanostructures fabricated from resist pyrolysis as a conducting channel. The carbon nanostructures are connected to source and drain electrodes. The device, except for the carbon channels, is covered with a passivation layer to protect the metal electrodes against electrolytes and to reduce nonspecific binding. When target molecules (streptavidin) bind with receptor molecules (biotin) on the carbon nanowire channel, channel conductance is varied by the charges of the target molecules.

Fig. 2 shows the fabrication processes of nanoscale carbon devices for biosensing applications. The fabrication process starts onto a 4" Si P (100) wafer with 0.8  $\mu\text{m}$ -thick  $\text{SiO}_2$ . A 70 nm-thick Au layer over a 10 nm-thick Cr layer, for aligning markers for electron beam lithography and source/drain electrodes, was delineated using the lift-off technique. A negative electron beam resist, SAL-601, was spin-coated onto the wafer at 5000 rpm for 35 sec, followed by soft-bake on a hotplate at 170  $^\circ\text{C}$  for 3 min.

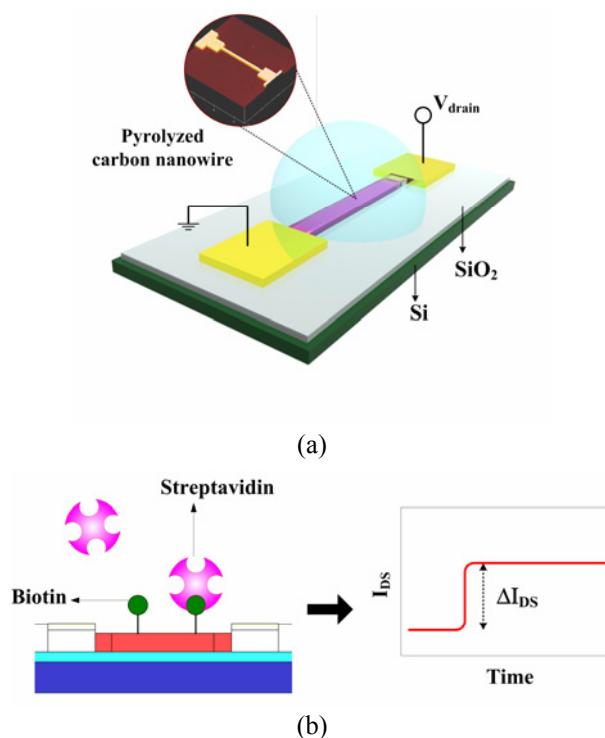


Fig. 1 Schematics of (a) an electrical biosensor utilizing carbon nanostructures fabricated from resist pyrolysis as a conducting channel and (b) variations of source-to-drain current  $I_{\text{DS}}$  (right) due to streptavidin binding with biotin on carbon channels (left).

Electron beam resist patterns were fabricated through exposures at 30 keV energy, 0.2-1  $\mu\text{C}/\text{cm}^2$  doses, and development with AZ300MIF for 5 min. After resist patterning using electron beam lithography, carbon patterns were obtained by resist pyrolysis. Electron beam exposures for metal contacts were carried out at 30 keV energy with a 100  $\text{C}/\text{cm}^2$  dose using 950K 4 wt.% PMMA. After development, carbon nanopatterns were connected to source and drain electrodes via the Au/Cr layer through the lift-off technique. PMMA passivations followed in order to shield metal electrodes from liquids. Suspended carbon mechanical nanostructures were fabricated by etching the underlying oxide layer using buffered HF.

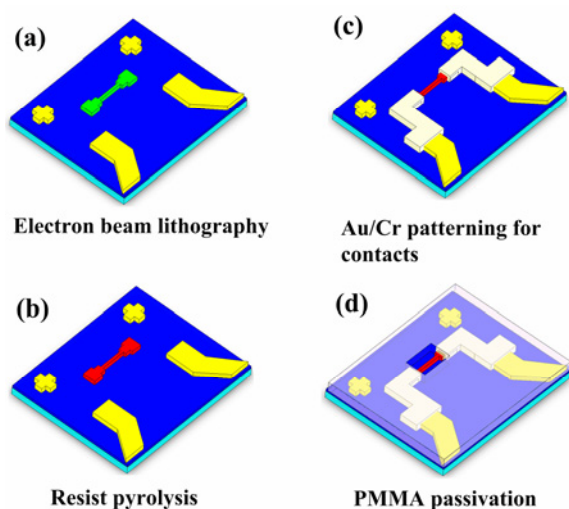


Fig. 2 Fabrication processes of carbon nanodevices for biosensing applications.

## 2.2 Biotin immobilization

After PMMA passivation, the device was  $\text{O}_2$  plasma-treated at 150 mTorr and 50 W for 15 sec to increase the density of oxygen-containing functional groups on the surface of the carbon nanowires. A reservoir was formed using a silicone tube with an inner diameter of 3 mm. By curing a 10:1 mixture of PDMS (Sylgard 184, Dow Corning) at 60  $^\circ\text{C}$  for 8 hr as a glue, the silicone tube was sealed to the device chip. Electrical characteristics such as source-drain current, gate-voltage responses, and pH dependences were measured using a semiconductor parameter analyzer (HP4156A).

Streptavidin (Sigma), which has a high binding affinity to biotin, was employed as a model protein to demonstrate the utility of carbon nanowires in the proposed biosensor. Biotin, as a receptor for the streptavidin binding measurement, was immobilized on the carbon nanowires. The carbon nanowires were incubated in 100 ml ethanol with 50 mM 1-ethyl-3-(3-

dimethylaminopropyl) carbodiimide hydrochloride (EDC) and 50 mM N-hydroxysuccinimide (NHS) for 2 hr, and were then rinsed with ethanol. The carbon nanowires were kept in 100 ml ethanol with 1 mg/ml biotin (EZ-Link amine- $\text{PEO}_2$ -biotin) for 2 hr and were then rinsed thoroughly with ethanol and PBS solution (pH 7.4), respectively. The carboxyl ( $\text{COOH}$ ) groups on the surface of the carbon nanowires were transformed using EDC/NHS into intermediates that readily react with the  $\text{NH}_2$  groups on biotin. The biotin was immobilized onto the surface of the carbon nanowires using an amide bond.

## 3. Results

### 3.1 Carbon nanofabrication

Fig. 3(a) shows the thickness and surface roughness of SAL-601 patterned using different exposure doses. As exposure dose increases, proximity effects and the molecular weight of the resist also increase due to higher monomer cross-linking. As the dose increased from 0.2  $\text{C}/\text{cm}^2$  to 1  $\text{C}/\text{cm}^2$ , the patterned resist thickness increased from 98 nm to 108 nm, and the surface roughness decreased from 3.4 nm to 2.2 nm. Fig. 3(b) shows an example of free-style resist nanopatterns fabricated using a 1  $\text{C}/\text{cm}^2$  dose, which contains 65 nm radius dots. Pattern widening and resist residues due to proximity effects were observed in the case of nanopatterns fabricated using a 1  $\text{C}/\text{cm}^2$  dose (fig. 3b).

Free-style resist nanopatterns were fabricated using a low dose of 0.2  $\text{C}/\text{cm}^2$  to reduce pattern widening and resist residues, which were subjected to heat treatment to obtain the intended carbon nanopatterns. Various carbon nanostructures, such as nanowires, nanodots, and suspended nanobridges, were fabricated using this method as shown in Fig. 4. Because carbon geometry is defined by the lithography process, we can fabricate free-shaped carbon devices (fig. 4a) and 3D mechanical nanostructures (fig. 4b). After PMMA passivation to protect the metal electrodes from oxide etchant (fig. 2d), the underlying oxide was wet-etched using buffered oxide etchant for 3 min. The released carbon nanostructures were rinsed with deionized water and methanol and allowed to dry.

Fig. 4b shows 122 nm-wide, 15 nm-thick, and 2  $\mu\text{m}$ -long carbon nanobridges suspended from a silicon substrate fabricated using carbon nanofabrication and underlying oxide etching. Fabricated carbon nanostructures show tensile stresses, useful for mechanical elements such as membranes and bridges, which are formed due to resist shrinkage and out-gassing during pyrolysis. The carbon nanobridges can be used as resonant sensors for miniscule force or mass detection.

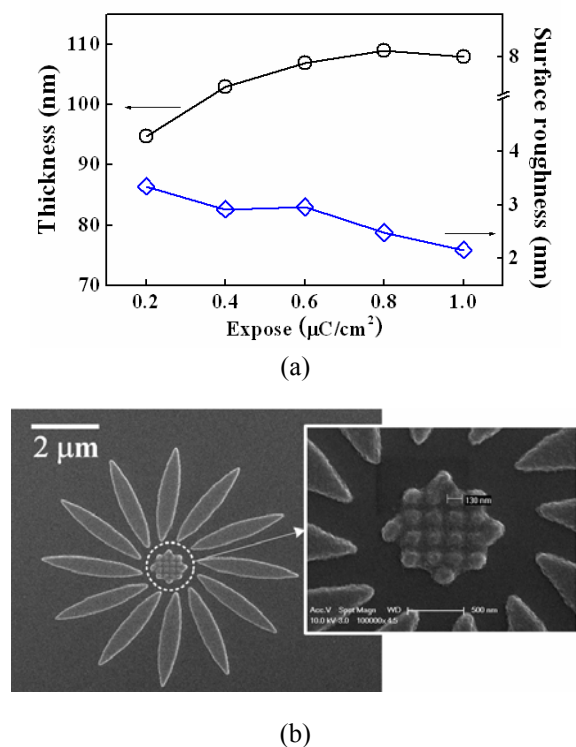


Fig. 3 (a) Negative electron beam resist (SAL-601) pattern thickness and surface roughness variations according to exposure doses between 0.2  $\text{C}/\text{cm}^2$  and 1  $\text{C}/\text{cm}^2$  and (b) An example of fabricated resist patterns using a high dose of 1  $\text{C}/\text{cm}^2$ .

Suspended nanostructures, which have a larger surface-to-volume ratio (a factor of two) compared to nanowires with similar dimensions, will be useful for surface-sensitive devices such as gas sensors and biosensors.

The thickness and surface roughness changes of carbon nanostructures compared to initial resist nanopatterns were measured by atomic force microscopy (AFM, Dimension<sup>TM</sup> 3100, Digital Instruments). The carbon nanowire thickness fabricated by resist pyrolysis was 25 nm, whereas the initial resist thickness was 100 nm. Carbon thicknesses after pyrolysis were varied by process conditions such as initial resist thickness, exposure doses, and oxidizing gas ratios. Thicker carbon nanostructures were thinned down by oxygen plasma treatment. Resist residues or scum were also removed by oxygen plasma. After etching of the carbon nanostructures with oxygen plasma at 50 W for 45 sec, the thickness of carbon nanostructures was decreased to 10.4 nm from an initial thickness of 14.3 nm, whereas the surface roughness was slightly increased to 0.61 nm from an initial roughness of 0.57 nm.

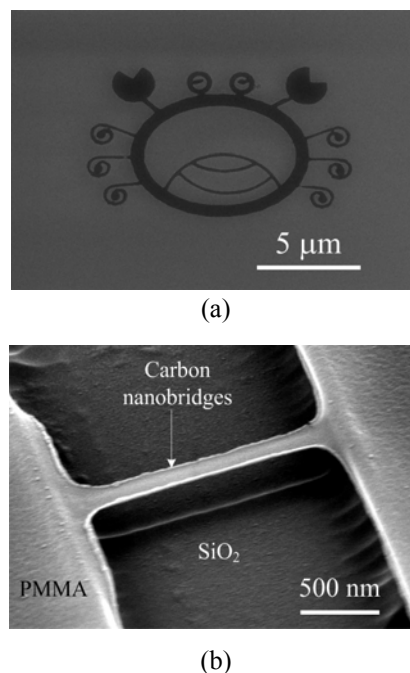


Fig. 4 SEM photomicrographs of fabricated carbon nanostructures using electron beam lithography and resist pyrolysis. (a)-(c) are free-handed carbon nanostructures and (d) shows carbon nanobridges suspended over silicon substrate.

Fig. 5 shows thickness and resistivity variations according to pyrolysis temperatures between 640  $^{\circ}\text{C}$  and 760  $^{\circ}\text{C}$  for carbon layers fabricated using SAL-601. Carbon thickness and resistivity were measured by AFM and the van der Pauw method using Greek cross test patterns, respectively. The thickness of the carbon layer obtained after pyrolysis was between 15 and 21 nm, which was 16-25% of the initial resist thickness of 80-110 nm. The resistivity of the carbon layer was between 5.2  $\Omega\cdot\text{cm}$  and 0.75  $\Omega\cdot\text{cm}$  and decreased as pyrolysis temperature increased. Black, opaque, smooth carbon surfaces, with a root mean square (rms) roughness below 0.6 nm and indistinguishable top- and bottom-sides, were obtained using mirror-polished silicon substrates and slow out-gassing during heat treatment. For carbon patterns pyrolyzed at 700  $^{\circ}\text{C}$ , a weak p-type majority conduction carrier with a Hall coefficient of 0.44  $\text{cm}^3/\text{C}$  was measured by Hall measurement system (HL5500PC).

### 3.2 Streptavidin detection

We studied applications of carbon nanostructures to active channels in electrical biosensors. For biosensing applications, we used carbon nanostructures pyrolyzed at 700  $^{\circ}\text{C}$  because of their intermediate conductivity of a few  $\Omega\cdot\text{cm}$  and to avoid excess carrier density.

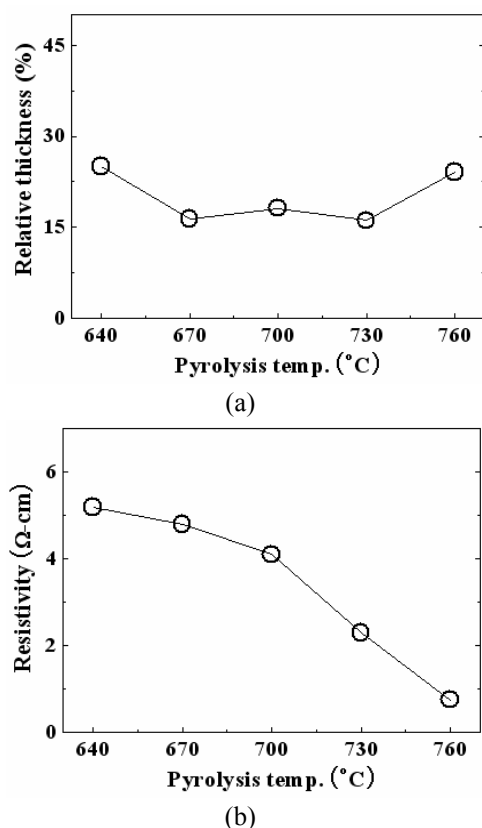


Fig. 5. (a) relative thickness and (b) resistivity of the pyrolyzed carbon as a function of pyrolysis temperature.

Carbon nanostructures containing 20 nm-thick, 130 nm-wide, and 4  $\mu\text{m}$ -thick carbon nanowires were used as conducting channels in the electrical biosensors. Fig. 6 shows measurements of source-to-drain current  $I_{\text{DS}}$  versus time for  $V_{\text{DS}}=300$  mV after introduction of 0.5 mg/ml streptavidin in 10 mM PBS solution (pH 7.4). The source-to-drain current  $I_{\text{DS}}$  of the biotin-modified carbon nanowire device was increased after streptavidin injection. The increase in  $I_{\text{DS}}$  after streptavidin introduction can be explained by the effect of negative gate voltages, which are induced by the negative charges of streptavidin (pI=5) bound with biotin on the carbon nanowires. The increase in  $I_{\text{DS}}$  after streptavidin introduction was consistent with the results of the Hall measurements showing p-type majority conduction behaviors of the carbon nanostructures.

As a control experiment (inset in Fig. 6), streptavidin was introduced to biotin-unmodified carbon nanowire devices. After introduction of 0.5 mg/ml streptavidin in 10 mM PBS solution,  $I_{\text{DS}}$  values for biotin-unmodified control devices were not changed after streptavidin injection. We believe that the gate voltage responses can be further improved by modifying microstructures of the carbon channel.

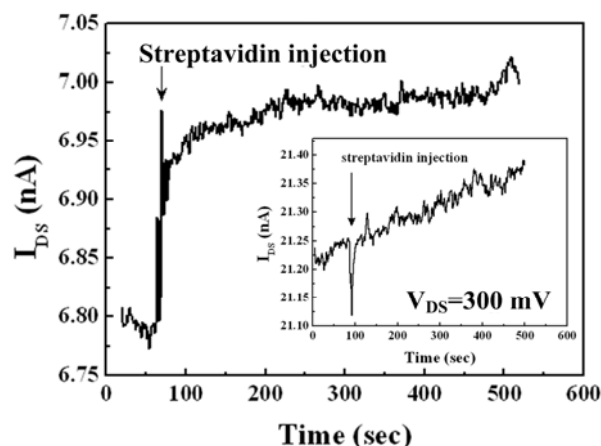


Fig. 6. Source-to-drain current,  $I_{\text{DS}}$ , versus time after streptavidin injection onto biotin-grafted device ( $V_{\text{DS}} = 300$  mV,  $\downarrow$ : streptavidin injection) (Inset: A control experiment onto biotin-untreated device),

#### 4. Conclusions

We fabricated free-style, free-standing carbon nanostructures, including nanodots, nanowires, and suspended nanobridges, using resist pyrolysis and nanomachining processes. Resist patterns were fabricated using a negative electron beam resist, SAL-601, and a modified scanning electron microscope. Carbon nanostructures were fabricated by thermal treatment of the resist patterns in a nitrogen atmosphere at temperatures between 640  $^{\circ}\text{C}$  and 760  $^{\circ}\text{C}$ . Suspended carbon nanobridges were fabricated by wet-etching of the underlying oxide. Electrical biosensors were fabricated by utilizing the carbon nanostructures as conducting channels. Conductances of the carbon nanowire channels were increased after streptavidin injection onto the biotin-grafted devices.

We expect that the carbon nanofabrication method (which relies on resist pyrolysis and a nanomachining process) and the resulting freestanding carbon nanostructures will be useful for various nanoscale sensors, including resonant sensors (mass, force, etc.) and biosensors.

#### References

- [1] Fritz, J., Baller, M. K., Lang, H. P., Rothuizen, H., Vettiger, P., Meyer, E., Güntherodt, H.-J., Gerber, Ch. and Gimzewski, J. K., 2000, "Translating biomolecular recognition into nanomechanics," *Science*, Vol. 288, pp. 316~318.
- [2] Shekhawat, G., Tark, S.-H. and Dravid, V. P., 2006, "MOSFET-embedded microcantilevers for measuring

- deflection in biomolecular sensors,” *Science*, Vol. 311 pp. 1592~1595
- [3] Truitt, P. A., Hertzberg, J. B., Huang, C. C., Ekinici, K. L. and Schwab, K. C., 2007, “Efficient and sensitive capacitive readout of nanomechanical resonator arrays,” *Nano Lett.*, Vol. 7 pp. 120~126.
- [4] Liu, H., Kameoka, J., Czaplewski, D. A. and Craighead, H. G., 2004, “Polymeric nanowire chemical sensor,” *Nano Lett.*, Vol. 4 pp. 671~675.
- [5] Kong, J., Franklin, N. R., Zhou, C., Chapline, M. G., Peng, S., Cho, K. and Dai, H., 2000, “Nanotube molecular wires as chemical sensors,” *Science*, Vol. 287 pp. 622~625.
- [6] Li, Z., Chen, Y., Li, X., Kamins, T. I., Nauka, K. and Williams, R. S., 2004, “Sequence-specific label-free DNA sensors based on silicon nanowires,” *Nano Lett.*, Vol. 4 pp. 245~247.
- [7] Kim, J., Song, X., Kinoshita, K., Madou, M. and White, R., 1998, “Electrochemical studies of carbon films from pyrolyzed photoresist,” *J. Electrochem. Soc.*, Vol. 145 pp. 2314~2319.
- [8] Schueller, O. J. A., Brittain, S. T. and Whitesides, G. M., 1999, “Fabrication of glassy carbon microstructures by soft lithography,” *Sens. Actuators A*, Vol. 72 pp. 125~139.
- [9] Lee, J. A., Lee, S. W., Lee, K.-C., Park, S. I. and Lee, S. S., 2008, “Fabrication and characterization of freestanding 3D carbon microstructures using multi-exposure and resist pyrolysis,” *J. Micromech. Microeng.*, Vol. 18 pp. 035012.